January 2008

Search for the lightest scalar top quark in events with two leptons in *pp* collisions at √s = 1.96 TeV

V. M. Abazov
Joint Institute for Nuclear Research, Dubna, Russia

Kenneth A. Bloom
University of Nebraska-Lincoln, kenbloom@unl.edu

Gregory Snow
University of Nebraska-Lincoln, gsnow1@unl.edu

D0 Collaboration

Available online at www.sciencedirect.com
ScienceDirect
Physics Letters B 659 (2008) 500–508
PHYSICS LETTERS B
www.elsevier.com/locate/physletb

Search for the lightest scalar top quark in events with two leptons in $p\bar{p}$ collisions at $\sqrt{s} = 1.96$ TeV

DØ Collaboration

V.M. Abazov [ai], B. Abbott [bw], M. Abolins [bm], B.S. Acharya [ab], M. Adams [ay], T. Adams [aw], E. Aguilo [e], S.H. Ahn [ad], M. Ahsan [bg], G.D. Alexeev [ai], G. Alkhazov [am], A. Alton [bl,1], G. Alverson [bk], G.A. Alves [b], M. Anastasoaie [ah], L.S. Ancu [ah], T. Andeen [ba], S. Anderson [as], B. Andrieu [p], M.S. Anzelc [ba], Y. Arnoud [m], M. Arov [bh], M. Arthaud [q], A. Askew [aw], B. Åsman [an], A.C.S. Assis Jesus [c], O. Atramentov [aw], C. Autermann [t], C. Avila [g], C. Ay [w], F. Badaud [l], A. Baden [bi], L. Bagby [az], B. Baldin [ax], D.V. Bandurin [bg], S. Banerjee [ab], P. Banerjee [ab], E. Barberis [bk], A.-F. Barfuss [n], P. Bargassa [cb,*], P. Baringer [bf], J. Barreto [b], J.F. Bartlett [ax], U. Bassler [p], D. Bauer [aq], S. Beale [e], A. Bean [bf], M. Begalli [c], M. Begel [bs], C. Belanger-Champagne [an], L. Bellantoni [ax], A. Bellavance [ax], J.A. Benitez [bm], S.B. Beri [z], G. Bernardi [p], R. Bernhard [v], L. Berntzon [n], I. Bertram [ap], M. Besançon [q], R. Beuselinck [aq], V.A. Bezzubov [al], P.C. Bhat [ax], V. Bhatnagar [z], C. Biscarat [s], G. Blazey [az], F. Blekman [aq], S. Blessing [aw], D. Bloch [r], K. Bloom [bo], A. Boehnlein [ax], D. Boline [bj], T.A. Bolton [bg], G. Borissov [ap], K. Bos [ag], T. Bose [by], A. Brandt [bz], R. Brock [bm], G. Brooijmans [br], A. Bross [ax], D. Brown [bz], N.J. Buchanan [aw], D. Buchholz [ba], M. Buehler [cc], V. Buescher [u], S. Burdin [ap,2], S. Burke [as], T.H. Burnett [cd], C.P. Buszello [aq], J.M. Butler [bj], P. Calfayan [x], S. Calvet [n], J. Cammin [bs], S. Caron [ag], W. Carvalho [c], B.C.K. Casey [by], N.M. Cason [bc], H. Castilla-Valdez [af], S. Chakrabarti [q], D. Chakraborty [az], K.M. Chan [bc], K. Chan [e], A. Chandra [av], F. Charles [r,✠], E. Cheu [as], F. Chevallier [m], D.K. Cho [bj], S. Choi [ae], B. Choudhary [aa], L. Christofek [by], T. Christoudias [aq,3], S. Cihangir [ax], D. Claes [bo], B. Clément [r], Y. Coadou [e], M. Cooke [cb], W.E. Cooper [ax], M. Corcoran [cb], F. Couderc [q], M.-C. Cousinou [n], S. Crépé-Renaudin [m], D. Cutts [by], M. Ćwiok [ac], H. da Motta [b], A. Das [bj], G. Davies [aq], K. De [bz], S.J. de Jong [ah], P. de Jong [ag], E. De La Cruz-Burelo [bl], C. De Oliveira Martins [c], J.D. Degenhardt [bl], F. Déliot [q], M. Demarteau [ax], R. Demina [bs], D. Denisov [ax], S.P. Denisov [al], S. Desai [ax], H.T. Diehl [ax], M. Diesburg [ax], A. Dominguez [bo], H. Dong [bt], L.V. Dudko [ak], L. Duflot [o], S.R. Dugad [ab], D. Duggan [aw], A. Duperrin [n], J. Dyer [bm], A. Dyshkant [az], M. Eads [bo], D. Edmunds [bm], J. Ellison [av], V.D. Elvira [ax], Y. Enari [by], S. Eno [bi], P. Ermolov [ak], H. Evans [bb], A. Evdokimov [bu], V.N. Evdokimov [al], A.V. Ferapontov [bg], T. Ferbel [bs], F. Fiedler [x], F. Filthaut [ah], W. Fisher [ax], H.E. Fisk [ax], M. Ford [ar], M. Fortner [az], H. Fox [v], S. Fu [ax], S. Fuess [ax], T. Gadfort [cd], C.F. Galea [ah], E. Gallas [ax], E. Galyaev [bc], C. Garcia [bs], A. Garcia-Bellido [cd], V. Gavrilov [aj], P. Gay [l], W. Geist [r], D. Gelé [r], C.E. Gerber [ay], Y. Gershtein [aw], D. Gillberg [e], G. Ginther [bs], N. Gollub [an], B. Gómez [g], A. Goussiou [bc], P.D. Grannis [bt], H. Greenlee [ax], Z.D. Greenwood [bh], E.M. Gregores [d], G. Grenier [s], Ph. Gris [l], J.-F. Grivaz [o], A. Grohsjean [x], S. Grünendahl [ax], M.W. Grünewald [ac], J. Guo [bt], F. Guo [bt], P. Gutierrez [bw], G. Gutierrez [ax], A. Haas [br], N.J. Hadley [bi], P. Haefner [x], S. Hagopian [aw], J. Haley [bp], I. Hall [bm], R.E. Hall [au], L. Han [f], K. Hanagaki [ax], P. Hansson [an], K. Harder [ar], A. Harel [bs], R. Harrington [bk], J.M. Hauptman [be], R. Hauser [bm], J. Hays [aq], T. Hebbeker [t], D. Hedin [az],

0370-2693/$ – see front matter
doi:10.1016/j.physletb.2007.11.086

J.G. Hegeman [ag], J.M. Heinmiller [ay], A.P. Heinson [av], U. Heintz [bj], C. Hensel [bf], K. Herner [bt], G. Hesketh [bk], M.D. Hildreth [bc], R. Hirosky [cc], J.D. Hobbs [bt], B. Hoeneisen [k], H. Hoeth [y], M. Hohlfeld [u], S.J. Hong [ad], R. Hooper [by], S. Hossain [bw], P. Houben [ag], Y. Hu [bt], Z. Hubacek [i], V. Hynek [h], I. Iashvili [bq], R. Illingworth [ax], A.S. Ito [ax], S. Jabeen [bj], M. Jaffré [o], S. Jain [bw], K. Jakobs [v], C. Jarvis [bi], R. Jesik [aq], K. Johns [as], C. Johnson [br], M. Johnson [ax], A. Jonckheere [ax], P. Jonsson [aq], A. Juste [ax], D. Käfer [t], S. Kahn [bu], E. Kajfasz [n], A.M. Kalinin [ai], J.R. Kalk [bm], J.M. Kalk [bh], S. Kappler [t], D. Karmanov [ak], J. Kasper [bj], P. Kasper [ax], I. Katsanos [br], D. Kau [aw], R. Kaur [z], V. Kaushik [bz], R. Kehoe [ca], S. Kermiche [n], N. Khalatyan [al], A. Khanov [bx], A. Kharchilava [bq], Y.M. Kharzheev [ai], D. Khatidze [br], H. Kim [ae], T.J. Kim [ad], M.H. Kirby [ah], M. Kirsch [t], B. Klima [ax], J.M. Kohli [z], J.-P. Konrath [v], M. Kopal [bw], V.M. Korablev [al], A.V. Kozelov [al], D. Krop [bb], A. Kryemadhi [cc], T. Kuhl [w], A. Kumar [bq], S. Kunori [bi], A. Kupco [j], T. Kurča [s], J. Kvita [h], F. Lacroix [l], D. Lam [bc], S. Lammers [br], G. Landsberg [by], J. Lazoflores [aw], P. Lebrun [s], W.M. Lee [ax], A. Leflat [ak], F. Lehner [ao], J. Lellouch [p], J. Leveque [as], P. Lewis [aq], J. Li [bz], Q.Z. Li [ax], L. Li [av], S.M. Lietti [d], J.G.R. Lima [az], D. Lincoln [ax], J. Linnemann [bm], V.V. Lipaev [al], R. Lipton [ax], Y. Liu [f,3], Z. Liu [e], L. Lobo [aq], A. Lobodenko [am], M. Lokajicek [j], A. Lounis [r], P. Love [ap], H.J. Lubatti [cd], A.L. Lyon [ax], A.K.A. Maciel [b], D. Mackin [cb], R.J. Madaras [at], P. Mättig [y], C. Magass [t], A. Magerkurth [bl], N. Makovec [o], P.K. Mal [bc], H.B. Malbouisson [c], S. Malik [bo], V.L. Malyshev [ai], H.S. Mao [ax], Y. Maravin [bg], B. Martin [m], R. McCarthy [bt], A. Melnitchouk [bn], A. Mendes [n], L. Mendoza [g], P.G. Mercadante [d], M. Merkin [ak], K.W. Merritt [ax], J. Meyer [u], A. Meyer [t], M. Michaut [q], T. Millet [s], J. Mitrevski [br], J. Molina [c], R.K. Mommsen [ar], N.K. Mondal [ab], R.W. Moore [e], T. Moulik [bf], G.S. Muanza [s], M. Mulders [ax], M. Mulhearn [br], O. Mundal [u], L. Mundim [c], E. Nagy [n], M. Naimuddin [ax], M. Narain [by], N.A. Naumann [ah], H.A. Neal [bl], J.P. Negret [g], P. Neustroev [am], H. Nilsen [v], A. Nomerotski [ax], S.F. Novaes [d], T. Nunnemann [x], V. O'Dell [ax], D.C. O'Neil [e], G. Obrant [am], C. Ochando [o], D. Onoprienko [bg], N. Oshima [ax], J. Osta [bc], R. Otec [i], G.J. Otero y Garzón [ay], M. Owen [ar], P. Padley [cb], M. Pangilinan [by], N. Parashar [bd], S.-J. Park [bs], S.K. Park [ad], J. Parsons [br], R. Partridge [by], N. Parua [bb], A. Patwa [bu], G. Pawloski [cb], B. Penning [v], K. Peters [ar], Y. Peters [y], P. Pétroff [o], M. Petteni [aq], R. Piegaia [a], J. Piper [bm], M.-A. Pleier [u], P.L.M. Podesta-Lerma [af,4], V.M. Podstavkov [ax], Y. Pogorelov [bc], M.-E. Pol [b], P. Polozov [aj], A. Pompoš, B.G. Pope [bm], A.V. Popov [al], C. Potter [e], W.L. Prado da Silva [c], H.B. Prosper [aw], S. Protopopescu [bu], J. Qian [bl], A. Quadt [u,5], B. Quinn [bn], A. Rakitine [ap], M.S. Rangel [b], K. Ranjan [aa], P.N. Ratoff [ap], P. Renkel [ca], S. Reucroft [bk], P. Rich [ar], M. Rijssenbeek [bt], I. Ripp-Baudot [r], F. Rizatdinova [bx], S. Robinson [aq], R.F. Rodrigues [c], C. Royon [q], P. Rubinov [ax], R. Ruchti [bc], G. Safronov [aj], G. Sajot [m], A. Sánchez-Hernández [af], M.P. Sanders [p], A. Santoro [c], G. Savage [ax], L. Sawyer [bh], T. Scanlon [aq], D. Schaile [x], R.D. Schamberger [bt], Y. Scheglov [am], H. Schellman [ba], P. Schieferdecker [x], T. Schliephake [y], C. Schwanenberger [ar], A. Schwartzman [bp], R. Schwienhorst [bm], J. Sekaric [aw], S. Sengupta [aw], H. Severini [bw], E. Shabalina [ay], M. Shamim [bg], V. Shary [q], A.A. Shchukin [al], R.K. Shivpuri [aa], D. Shpakov [ax], V. Siccardi [r], V. Simak [i], V. Sirotenko [ax], P. Skubic [bw], P. Slattery [bs], D. Smirnov [bc], J. Snow [bv], G.R. Snow [bo], S. Snyder [bu], S. Söldner-Rembold [ar], L. Sonnenschein [p], A. Sopczak [ap], M. Sosebee [bz], K. Soustruznik [h], M. Souza [b], B. Spurlock [bz], J. Stark [m], J. Steele [bh], V. Stolin [aj], A. Stone [ay], D.A. Stoyanova [al], J. Strandberg [bl], S. Strandberg [an], M.A. Strang [bq], M. Strauss [bw], E. Strauss [bt], R. Ströhmer [x], D. Strom [ba], L. Stutte [ax], S. Sumowidagdo [aw], P. Svoisky [bc], A. Sznajder [c], M. Talby [n], P. Tamburello [as], A. Tanasijczuk [a], W. Taylor [e], P. Telford [ar], J. Temple [as], B. Tiller [x], F. Tissandier [l], M. Titov [q], V.V. Tokmenin [ai], T. Toole [bi], I. Torchiani [v], T. Trefzger [w], D. Tsybychev [bt], B. Tuchming [q], C. Tully [bp], P.M. Tuts [br], R. Unalan [bm], S. Uvarov [am], L. Uvarov [am], S. Uzunyan [az], B. Vachon [e],

P.J. van den Berg [ag], B. van Eijk [ag], R. Van Kooten [bb], W.M. van Leeuwen [ag], N. Varelas [ay], E.W. Varnes [as], I.A. Vasilyev [al], M. Vaupel [y], P. Verdier [s], L.S. Vertogradov [ai], M. Verzocchi [ax], F. Villeneuve-Seguier [aq], P. Vint [aq], P. Vokac [i], E. Von Toerne [bg], M. Voutilainen [bo,6], M. Vreeswijk [ag], R. Wagner [bp], H.D. Wahl [aw], L. Wang [bi], M.H.L.S. Wang [ax], J. Warchol [bc], G. Watts [cd], M. Wayne [bc], M. Weber [ax], G. Weber [w], A. Wenger [v,7], N. Wermes [u], M. Wetstein [bi], A. White [bz], D. Wicke [y], G.W. Wilson [bf], S.J. Wimpenny [av], M. Wobisch [bh], D.R. Wood [bk], T.R. Wyatt [ar], Y. Xie [by], S. Yacoob [ba], R. Yamada [ax], M. Yan [bi], T. Yasuda [ax], Y.A. Yatsunenko [ai], K. Yip [bu], H.D. Yoo [by], S.W. Youn [ba], J. Yu [bz], A. Zatserklyaniy [az], C. Zeitnitz [y], D. Zhang [ax], T. Zhao [cd], B. Zhou [bl], J. Zhu [bt], M. Zielinski [bs], D. Zieminska [bb], A. Zieminski [bb], L. Zivkovic [br], V. Zutshi [az], E.G. Zverev [ak]

[a] *Universidad de Buenos Aires, Buenos Aires, Argentina*
[b] *LAFEX, Centro Brasileiro de Pesquisas Físicas, Rio de Janeiro, Brazil*
[c] *Universidade do Estado do Rio de Janeiro, Rio de Janeiro, Brazil*
[d] *Instituto de Física Teórica, Universidade Estadual Paulista, São Paulo, Brazil*
[e] *University of Alberta, Edmonton, Alberta, and Simon Fraser University, Burnaby, British Columbia, and York University, Toronto, Ontario, and McGill University, Montreal, Quebec, Canada*
[f] *University of Science and Technology of China, Hefei, People's Republic of China*
[g] *Universidad de los Andes, Bogotá, Colombia*
[h] *Center for Particle Physics, Charles University, Prague, Czech Republic*
[i] *Czech Technical University, Prague, Czech Republic*
[j] *Center for Particle Physics, Institute of Physics, Academy of Sciences of the Czech Republic, Prague, Czech Republic*
[k] *Universidad San Francisco de Quito, Quito, Ecuador*
[l] *Laboratoire de Physique Corpusculaire, IN2P3-CNRS, Université Blaise Pascal, Clermont-Ferrand, France*
[m] *Laboratoire de Physique Subatomique et de Cosmologie, IN2P3-CNRS, Universite de Grenoble 1, Grenoble, France*
[n] *CPPM, IN2P3-CNRS, Université de la Méditerranée, Marseille, France*
[o] *Laboratoire de l'Accélérateur Linéaire, IN2P3-CNRS et Université Paris-Sud, Orsay, France*
[p] *LPNHE, IN2P3-CNRS, Universités Paris VI and VII, Paris, France*
[q] *DAPNIA/Service de Physique des Particules, CEA, Saclay, France*
[r] *IPHC, Université Louis Pasteur et Université de Haute Alsace, CNRS, IN2P3, Strasbourg, France*
[s] *IPNL, Université Lyon 1, CNRS/IN2P3, Villeurbanne, France and Université de Lyon, Lyon, France*
[t] *III. Physikalisches Institut A, RWTH Aachen, Aachen, Germany*
[u] *Physikalisches Institut, Universität Bonn, Bonn, Germany*
[v] *Physikalisches Institut, Universität Freiburg, Freiburg, Germany*
[w] *Institut für Physik, Universität Mainz, Mainz, Germany*
[x] *Ludwig-Maximilians-Universität München, München, Germany*
[y] *Fachbereich Physik, University of Wuppertal, Wuppertal, Germany*
[z] *Panjab University, Chandigarh, India*
[aa] *Delhi University, Delhi, India*
[ab] *Tata Institute of Fundamental Research, Mumbai, India*
[ac] *University College Dublin, Dublin, Ireland*
[ad] *Korea Detector Laboratory, Korea University, Seoul, South Korea*
[ae] *SungKyunKwan University, Suwon, South Korea*
[af] *CINVESTAV, Mexico City, Mexico*
[ag] *FOM-Institute NIKHEF and University of Amsterdam/NIKHEF, Amsterdam, The Netherlands*
[ah] *Radboud University Nijmegen/NIKHEF, Nijmegen, The Netherlands*
[ai] *Joint Institute for Nuclear Research, Dubna, Russia*
[aj] *Institute for Theoretical and Experimental Physics, Moscow, Russia*
[ak] *Moscow State University, Moscow, Russia*
[al] *Institute for High Energy Physics, Protvino, Russia*
[am] *Petersburg Nuclear Physics Institute, St. Petersburg, Russia*
[an] *Lund University, Lund, and Royal Institute of Technology and Stockholm University, Stockholm, and Uppsala University, Uppsala, Sweden*
[ao] *Physik Institut der Universität Zürich, Zürich, Switzerland*
[ap] *Lancaster University, Lancaster, United Kingdom*
[aq] *Imperial College, London, United Kingdom*
[ar] *University of Manchester, Manchester, United Kingdom*
[as] *University of Arizona, Tucson, AZ 85721, USA*
[at] *Lawrence Berkeley National Laboratory and University of California, Berkeley, CA 94720, USA*
[au] *California State University, Fresno, CA 93740, USA*
[av] *University of California, Riverside, CA 92521, USA*
[aw] *Florida State University, Tallahassee, FL 32306, USA*
[ax] *Fermi National Accelerator Laboratory, Batavia, IL 60510, USA*
[ay] *University of Illinois at Chicago, Chicago, IL 60607, USA*
[az] *Northern Illinois University, DeKalb, IL 60115, USA*
[ba] *Northwestern University, Evanston, IL 60208, USA*

[bb] Indiana University, Bloomington, IN 47405, USA
[bc] University of Notre Dame, Notre Dame, IN 46556, USA
[bd] Purdue University Calumet, Hammond, IN 46323, USA
[be] Iowa State University, Ames, IA 50011, USA
[bf] University of Kansas, Lawrence, KS 66045, USA
[bg] Kansas State University, Manhattan, KS 66506, USA
[bh] Louisiana Tech University, Ruston, LA 71272, USA
[bi] University of Maryland, College Park, MD 20742, USA
[bj] Boston University, Boston, MA 02215, USA
[bk] Northeastern University, Boston, MA 02115, USA
[bl] University of Michigan, Ann Arbor, MI 48109, USA
[bm] Michigan State University, East Lansing, MI 48824, USA
[bn] University of Mississippi, University, MS 38677, USA
[bo] University of Nebraska, Lincoln, NE 68588, USA
[bp] Princeton University, Princeton, NJ 08544, USA
[bq] State University of New York, Buffalo, NY 14260, USA
[br] Columbia University, New York, NY 10027, USA
[bs] University of Rochester, Rochester, NY 14627, USA
[bt] State University of New York, Stony Brook, NY 11794, USA
[bu] Brookhaven National Laboratory, Upton, NY 11973, USA
[bv] Langston University, Langston, OH 73050, USA
[bw] University of Oklahoma, Norman, OH 73019, USA
[bx] Oklahoma State University, Stillwater, OH 74078, USA
[by] Brown University, Providence, RI 02912, USA
[bz] University of Texas, Arlington, TX 76019, USA
[ca] Southern Methodist University, Dallas, TX 75275, USA
[cb] Rice University, Houston, TX 77005, USA
[cc] University of Virginia, Charlottesville, VA 22901, USA
[cd] University of Washington, Seattle, WA 98195, USA

Received 19 July 2007; received in revised form 19 November 2007; accepted 29 November 2007

Available online 5 December 2007

Editor: L. Rolandi

Abstract

Data collected by the D0 detector at a $p\bar{p}$ center-of-mass energy of 1.96 TeV at the Fermilab Tevatron Collider have been used to search for pair production of the lightest supersymmetric partner of the top quark decaying into $b\ell\tilde{\nu}$. The search is performed in the $\ell\ell' = e\mu$ and $\mu\mu$ final states. No evidence for this process has been found in data samples of approximately 400 pb^{-1}. The domain in the $[M(\tilde{t}_1), M(\tilde{\nu})]$ plane excluded at the 95% C.L. is substantially extended by this search.

PACS: 14.80.Ly; 12.60.Jv

Supersymmetric theories [1] predict the existence of a scalar partner for each standard model fermion. Because of the large mass of the Standard Model top quark, the mixing between its chiral supersymmetric partners is the largest among all squarks; therefore the lightest supersymmetric partner of the top quark, $\tilde{t}_1$ (stop), might be the lightest squark. If the $\tilde{t}_1 \to b\ell\tilde{\nu}$ decay channel is kinematically accessible, it will be dominant [2] as long as the $\tilde{t}_1 \to b\tilde{\chi}_1^{\pm}$ and $\tilde{t}_1 \to t\tilde{\chi}_1^0$ channels are kinematically closed, where $\tilde{\chi}_1^{\pm}$ and $\tilde{\chi}_1^0$ are the lightest chargino and neutralino, respectively. In this Letter we present a search for stop pair production in $p\bar{p}$ collisions at 1.96 TeV with the D0 detector, where a virtual chargino $\tilde{\chi}^{\pm}$ decays into a lepton and a sneutrino, and where the sneutrino $\tilde{\nu}$, considered to be the next lightest supersymmetric particle, decays into a neutrino and the lightest neutralino $\tilde{\chi}_1^0$; in $p\bar{p}$ collisions, stop pairs are dominantly produced via the strong interaction in quark–antiquark annihilation and gluon fusion. We use the minimal supersymmetric Standard Model (MSSM) as the phenomenological framework for this search. We assume the branching ratio $\mathrm{Br}(\tilde{\chi}_1^{\pm} \to \ell\tilde{\nu}) = 1$ with equal sharing among all lepton flavors, and we consider only cases where $\ell = e, \mu$. For stop

* Corresponding author.
E-mail address: bargassa@cern.ch (P. Bargassa).
[1] Visitor from Augustana College, Sioux Falls, SD, USA.
[2] Visitor from The University of Liverpool, Liverpool, UK.
[3] Fermilab International Fellow.
[4] Visitor from ICN-UNAM, Mexico City, Mexico.
[5] Visitor from II. Physikalisches Institut, Georg-August-University Göttingen, Germany.
[6] Visitor from Helsinki Institute of Physics, Helsinki, Finland.
[7] Visitor from Universität Zürich, Zürich, Switzerland.
✠ Deceased.

pair production, we consider $b\bar{b}\ell\ell'\nu\bar{\nu}\tilde{\chi}_1^0\tilde{\chi}_1^0$ final states with $\ell\ell' = e^{\pm}\mu^{\mp}$ and $\ell\ell' = \mu^+\mu^-$ ($e\mu$ and $\mu\mu$ channels); the signal topology consists of two isolated leptons, missing transverse energy ($\not\!\!E_T$), and jets. D0 has also searched for scalar top in the charm jet final state [3].

The D0 detector [4] comprises a central tracking system surrounded by a liquid-argon sampling calorimeter and a system of muon detectors. Charged particles are reconstructed using a multi-layer silicon detector and eight double layers of scintillating fibers in a 2 T magnetic field produced by a superconducting solenoid. The calorimeter provides hermetic coverage up to pseudo-rapidities $|\eta| \simeq 4$ (where $\eta = -\log(\tan(\theta/2))$, and where θ is the polar angle with respect to the proton beam direction) in a semi-projective tower geometry with longitudinal segmentation. After passing through the calorimeter, muons are detected in the muon detector comprising three layers of tracking detectors and scintillation counters located inside and outside of 1.8 T iron toroids. Events containing electrons or muons are selected for off-line analysis by a trigger system. A set of dilepton triggers is used to tag the presence of electrons and muons based on their energy deposit in the calorimeter, hits in the muon detectors, and tracks in the tracking system.

Three-body decays of the $\tilde{t}_1$ are simulated using COMPHEP [5] and PYTHIA [6] for generation and hadronization respectively. Standard Model background processes are simulated using the PYTHIA and ALPGEN [7] Monte Carlo (MC) generators. These MC samples are generated using the CTEQ5L [8] parton distribution functions (PDF); they are normalized using next-to-leading order cross sections [9]. All generated events are passed through the full simulation of the detector geometry and response based on GEANT [10]. MC events are then reconstructed and analyzed with the same programs as used for the data.

Muons are reconstructed by finding tracks pointing to hit patterns in the muon system. Non-isolated muons are rejected by requiring the sum of the transverse momenta (p_T) of tracks inside a cone with $\Delta\mathcal{R} = \sqrt{(\Delta\phi)^2 + (\Delta\eta)^2} = 0.5$ (where ϕ is the azimuthal angle) around the muon direction, and the calorimeter energy in an annulus of size $0.1 < \Delta\mathcal{R} < 0.4$ around the muon to be less than 4 GeV/c and 4 GeV. Isolated electrons are selected based on their characteristic energy deposition in the calorimeter, their fraction of deposited energy in the electromagnetic portion of the calorimeter and their transverse shower profile inside a cone of radius $\Delta\mathcal{R} = 0.4$ around the direction of the electron; furthermore, it is required that a track points to the energy deposition in the calorimeter and that its momentum and the calorimeter energy are consistent with the same electron energy; an "electron-likelihood" is defined as a variable combining information from the energy deposition in the calorimeter and the associated track. Backgrounds from jets and photon conversions are further suppressed by requiring the tracks associated with the muons and electrons to each have at least one hit in the silicon detector. Jets are reconstructed from the energy deposition in calorimeter towers using the Run II cone algorithm [11] with radius $\Delta\mathcal{R} = 0.5$, and corrected for the jet energy scale (JES) [12]; in this search, jets are considered with $p_T > 15$ GeV/c. The $\not\!\!E_T$ is defined as the energy imbalance of all calorimeter cells in the plane transverse to the beam direction, and is corrected for the JES, the electromagnetic energy scale, and reconstructed muons. All efficiencies are measured with data [13].

In both $e\mu$ and $\mu\mu$ channels, the signal points $[M(\tilde{t}_1), M(\tilde{\nu})] = (110, 80)$ GeV/c^2 and $(145, 50)$ GeV/c^2, respectively referred as "soft" (point A) and "hard" (point B) signals, have been used to optimize the selection of signals of different kinematics because of different $\Delta m = M(\tilde{t}_1) - M(\tilde{\nu})$. The choice of these points was also motivated by the sensitivity of the D0 search during Run I [14]. The main background processes imitating the signal topology are Z/γ^*, WW, $t\bar{t}$ production, and multijet background. All but the latter are estimated with MC simulation. The multijet background is estimated from data. In the $e\mu$ channel, two samples each dominated by a different multijet background are obtained by inverting the muon isolation requirements, and by inverting the cut on the electron-likelihood; in the $\mu\mu$ channel, such a sample is obtained by selecting same-sign muon events. Factors normalizing each sample to the selection sample are also obtained from data, and applied to the background samples to obtain the multijet background estimation, this, at an early stage of the selection.

For the $e\mu$ channel, the integrated luminosity [15] of the data sample is (428 ± 28) pb^{-1}. The preselection is concluded by requiring the transverse momenta of the electron and muon (see Fig. 1(a) and (b)) to be greater than 10 and 8 GeV/c, respectively. In this final state, the data are dominated by the multijet and $Z/\gamma^* \to \tau\tau$ backgrounds. In these processes, poorly reconstructed leptons are correlated with $\not\!\!E_T$, giving rise to higher event populations at high and low values of the azimuthal angular difference between the leptons and the $\not\!\!E_T$, a low value of the angular difference for one lepton being correlated with a high value of the other. Taking advantage of a higher background contribution at low values of angular distributions, we require

$$\Delta\phi(\mu, \not\!\!E_T) > 0.4, \qquad \Delta\phi(e, \not\!\!E_T) > 0.4. \tag{1}$$

We require $\not\!\!E_T$ to be greater than 15 GeV to reduce contribution of both the multijet and $Z/\gamma^* \to \tau\tau$ backgrounds. To reject multijet events in which leptons are associated with a jet, we require the two leptons to be at a $\Delta\mathcal{R}$ distance greater than 0.5 from any reconstructed jet. To further reduce the multijet contribution, we require the z component of the origin of the highest transverse momentum muon track to be within four standard deviations σ from the z component of the primary vertex:

$$\begin{aligned} &\not\!\!E_T > 15 \text{ GeV}, \\ &\Delta\mathcal{R}\big[(e,\mu), \text{jet}\big] > 0.5, \\ &\big|z(\mu) - z(\text{p.v.})\big| < 4\sigma. \end{aligned} \tag{2}$$

To reduce the $Z/\gamma^* \to \tau\tau$ background, we cut on low values of the transverse mass of the muon and $\not\!\!E_T$ ($M_T(\mu, \not\!\!E_T)$, see Fig. 1(c)). To further reduce this background, we make use of the correlation between the angular differences $\Delta\phi(\mu, \not\!\!E_T)$ and $\Delta\phi(e, \not\!\!E_T)$, and require their sum (see Fig. 1(d)) to be greater than 2.9:

$$M_T(\mu, \not\!\!E_T) > 15 \text{ GeV}/c^2,$$

Table 1
$e\mu$ channel. Expected numbers of events in various background and signal channels, and number of observed events in data, at various selection levels. Statistical as well as systematic uncertainties from the JES correction are shown for the total background and signal

Selection	Background contributions				Total background	Data	Signal	
	Multijet	$Z/\gamma^* \to \ell\ell$	$t\bar{t}$	Diboson			Point A	Point B
Preselection	304.5	286.7	12.4	28.6	$632.3 \pm 19.5^{+0.0}_{-0.0}$	596	$65.9 \pm 2.4^{+0.0}_{-0.0}$	$26.6 \pm 0.7^{+0.0}_{-0.0}$
(1)	194.4	115.4	10.4	25.3	$345.4 \pm 15.0^{+0.7}_{-0.7}$	329	$54.1 \pm 2.2^{+0.0}_{-0.0}$	$22.7 \pm 0.7^{+0.0}_{-0.0}$
(2)	8.6	20.0	9.1	21.2	$58.9 \pm 3.8^{+2.2}_{-2.2}$	52	$31.6 \pm 1.7^{+0.8}_{-0.0}$	$19.0 \pm 0.6^{+0.0}_{-0.1}$
(3)	5.9	3.6	7.4	20.2	$37.1 \pm 2.7^{+0.9}_{-0.9}$	34	$26.0 \pm 1.5^{+0.3}_{-0.0}$	$17.3 \pm 0.6^{+0.2}_{-0.2}$

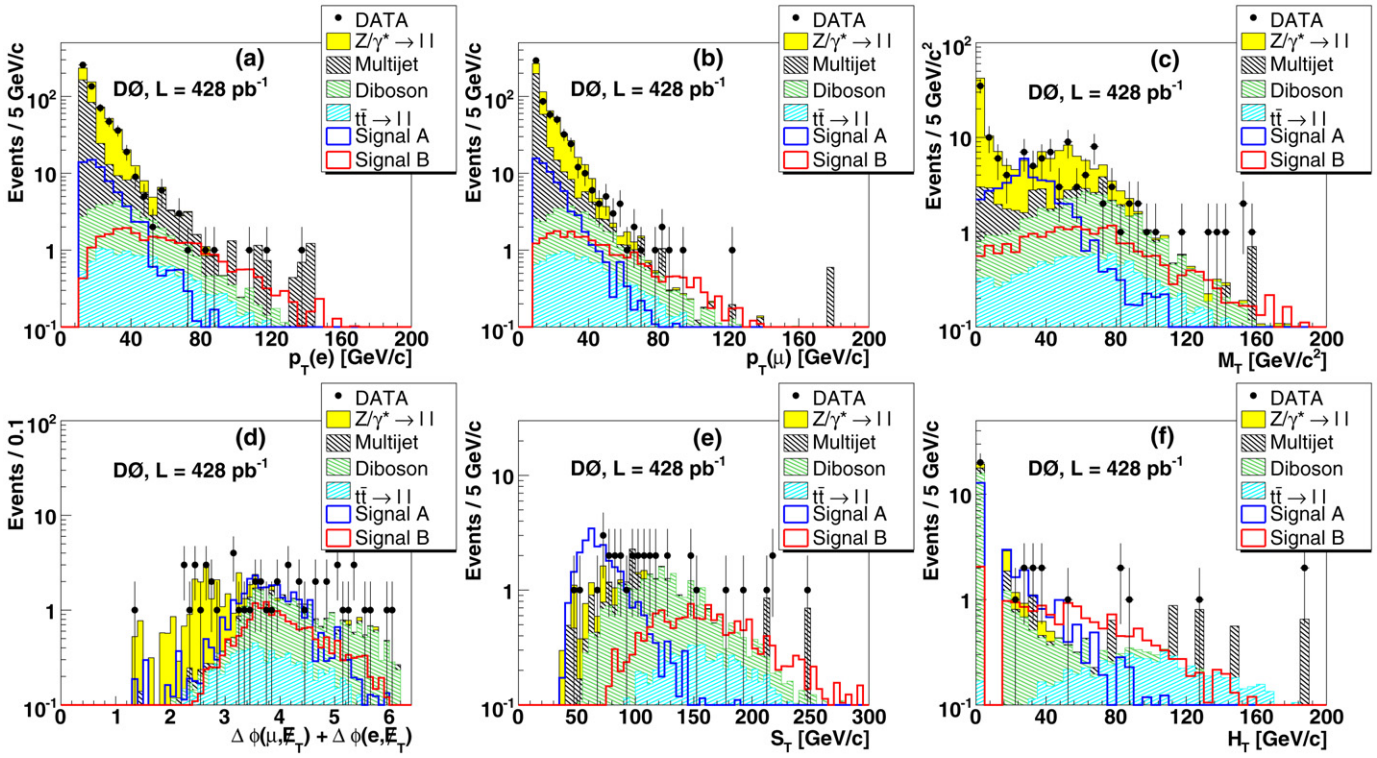

Fig. 1. $e\mu$ channel. Distributions of the transverse momenta of the electron (a) and of the muon (b) after preselection cuts; (c) the transverse mass $M_T(\mu, \not\!\!E_T)$ after preselection cuts and $\not\!\!E_T > 15$ GeV and $\Delta R[(e,\mu), \text{jet}] > 0.5$; (d) the angular sum $\Delta\phi(\mu, \not\!\!E_T) + \Delta\phi(e, \not\!\!E_T)$ after the cut (2); (e) S_T and (f) H_T distributions after the cut (3).

$$\Delta\phi(\mu, \not\!\!E_T) + \Delta\phi(e, \not\!\!E_T) > 2.9. \quad (3)$$

The contributions of different backgrounds, and the expected numbers of signal and observed data events in the $e\mu$ final state at different selection levels are summarized in Table 1. After all selections, the WW (dominating the diboson contribution) and $t\bar{t}$ contributions are the dominant backgrounds. To separate soft signals such as point A from these backgrounds, we consider the variable S_T defined as the scalar sum of the transverse momentum of the muon, the electron, and the $\not\!\!E_T$ (see Fig. 1(e)). To separate hard signals such as point B from background contributions, we consider the variable H_T defined as the scalar sum of the transverse momentum of all jets (see Fig. 1(f)). Rather than cutting on these two variables, the H_T and S_T spectra predicted for signal and background are compared with the observed spectra in twelve $[S_T, H_T]$ bins (see Table 2) when extracting limits on the signal cross section, thus allowing a separation of signals of different kinematics from the WW and $t\bar{t}$ backgrounds.

For the $\mu\mu$ channel, the integrated luminosity [15] of the data sample is (395 ± 26) pb^{-1}. The selection of the signal in this final state is more challenging because of the strongly dominating $Z/\gamma^* \to \mu\mu$ background. The preselection is concluded by requiring the transverse momenta of the two highest transverse momenta opposite-sign muons to be greater than 8 and 6 GeV/c. While the signal is characterized by the presence of jets originating from the hadronization of b quarks, the $Z/\gamma^* \to \mu\mu$ background owes the presence of jets to initial state radiation gluons which hadronize into softer jets, resulting in a lower multiplicity of jets; the latter is also valid for soft signals such as point A. To keep sensitivity to soft signals while rejecting substantial background, we require at least one jet:

$$N(\text{jets}) \geqslant 1. \quad (4)$$

Table 2
$e\mu$ channel. Expected numbers of events for total background, signal points A and B, and number of observed events in data, in the twelve $[S_T, H_T]$ bins. Statistical and JES uncertainties are added in quadrature for the total background and signal points

Bin	Total background	Data	Signal	
			Point A	Point B
$S_T \in [0, 70[$ GeV, $H_T = 0$	2.6 ± 1.1	1	7.3 ± 1.0	0.0 ± 0.0
$S_T \in [70, 120[$ GeV, $H_T = 0$	9.2 ± 1.2	14	4.8 ± 0.7	0.2 ± 0.1
$S_T \in [120, \ldots[$ GeV, $H_T = 0$	7.7 ± 0.7	5	0.8 ± 0.3	1.8 ± 0.2
$S_T \in [0, 70[$ GeV, $H_T \in]0, 60]$	1.9 ± 0.7	2	5.2 ± 0.7	0.0 ± 0.0
$S_T \in [70, 120[$ GeV, $H_T \in]0, 60]$	3.6 ± 1.2	4	5.3 ± 0.8	1.2 ± 0.2
$S_T \in [120, \ldots[$ GeV, $H_T \in]0, 60]$	3.0 ± 0.4	2	0.6 ± 0.3	6.3 ± 0.5
$S_T \in [0, 70[$ GeV, $H_T \in]60, 120]$	0.4 ± 0.6	0	0.6 ± 0.3	0.0 ± 0.0
$S_T \in [70, 120[$ GeV, $H_T \in]60, 120]$	0.7 ± 0.2	1	1.2 ± 0.3	1.3 ± 0.2
$S_T \in [120, \ldots[$ GeV, $H_T \in]60, 120]$	3.6 ± 0.8	2	0.1 ± 0.1	4.3 ± 0.3
$S_T \in [0, 70[$ GeV, $H_T \in]120, \ldots[$	0.0 ± 0.0	0	0.0 ± 0.0	0.0 ± 0.0
$S_T \in [70, 120[$ GeV, $H_T \in]120, \ldots[$	0.8 ± 0.6	1	0.0 ± 0.0	0.4 ± 0.1
$S_T \in [120, \ldots[$ GeV, $H_T \in]120, \ldots[$	3.7 ± 1.1	2	0.1 ± 0.1	1.7 ± 0.3

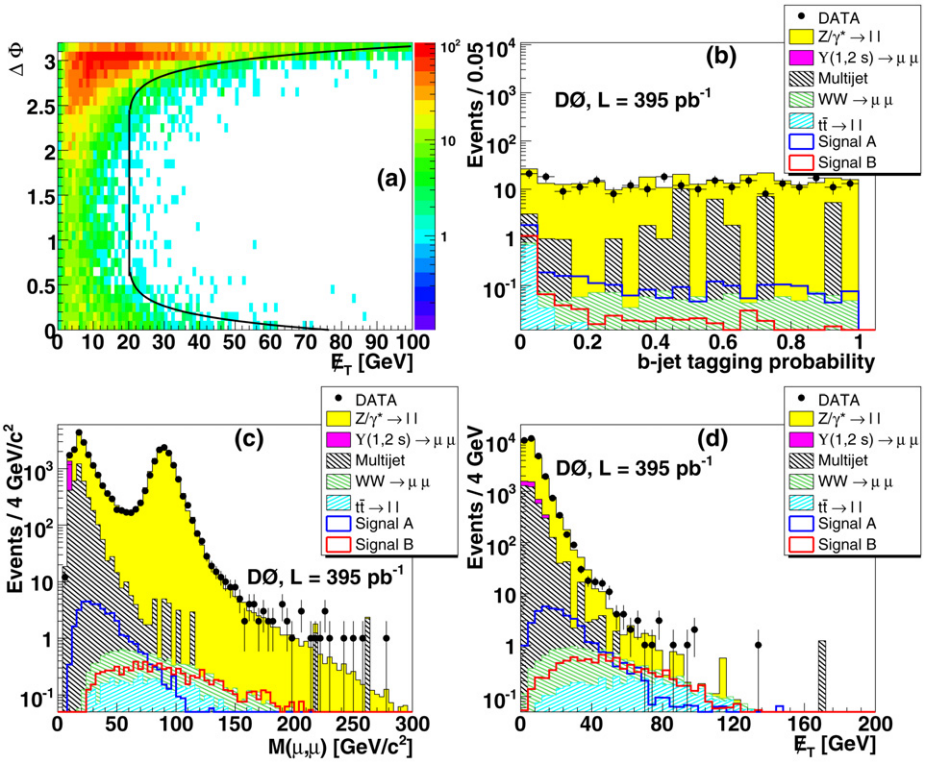

Fig. 2. $\mu\mu$ channel. (a) $\Delta\phi(\mu_1, \not\!\!E_T)$ versus $\not\!\!E_T$ in simulated $Z/\gamma^* \to \mu\mu$ events; the contour of the cut (5) is shown by the solid line. Distributions of the b jet tagging probability $\mathcal{P}$(jet) (b), the invariant mass of the two most energetic muons (c), and $\not\!\!E_T$ (d) after preselection cuts.

To further remove $Z/\gamma^* \to \mu\mu$ background events, where poorly reconstructed muons correlate with the $\not\!\!E_T$, we require the $\not\!\!E_T$ to be greater than the contour shown on Fig. 2(a), using a cut parametrized by the following equation:

$$\not\!\!E_T/\text{GeV} > 20 + \left|\Delta\phi(\mu_1, \not\!\!E_T) - 1.55\right|^{9.2}, \tag{5}$$

where μ_1 is the highest transverse momentum muon. To augment the search sensitivity in this channel, we take advantage of the presence of jets originating from the fragmentation of long-lived b quarks in the signal. An algorithm based on the lifetime of hadrons calculates the probability $\mathcal{P}$ for the tracks of a jet to originate from the primary interaction point [16]. This b jet tagging probability is constructed such that its distribution is uniform for light-flavor jets while peaking at zero for heavy-flavor jets which have a vertex significantly displaced from the primary vertex (Fig. 2(b)). Considering the highest transverse energy jet, we require

$$\mathcal{P}(\text{jet}) < 1\%. \tag{6}$$

A cut on the dimuon invariant mass (Fig. 2(c)) in the vicinity of the Z boson resonance only at low $\not\!\!E_T$ (Fig. 2(d)) further suppresses the $Z/\gamma^* \to \mu\mu$ background while preserving the signal:

$$M(\mu, \mu) \notin [75, 120]\ \text{GeV}/c^2 \quad \text{for } \not\!\!E_T < 50\ \text{GeV}. \tag{7}$$

Table 3
$\mu\mu$ channel. Expected numbers of events in various background and signal channels, and number of observed events in data, at various selection levels. Statistical as well as systematic uncertainties from the JES correction are shown for the total background and signal

Selection	Background contributions					Total background	Data	Signal	
	Multijet	$\Upsilon(1,2S)$	$Z/\gamma^* \to \ell\ell$	$t\bar{t}$	WW			Point A	Point B
Preselection	3607.6	973.1	23781.7	5.1	9.6	$28377.1 \pm 348^{+0.0}_{-0.0}$	28733	$9.8 \pm 0.4^{+0.0}_{-0.0}$	$41.1 \pm 1.5^{+0.0}_{-0.0}$
(4)	682.1	80.8	3894.9	5.1	1.5	$4664.4 \pm 97^{+452}_{-553}$	4337	$8.8 \pm 0.4^{+0.1}_{-0.1}$	$24.2 \pm 1.1^{+1.5}_{-1.9}$
(5)	41.8	0.4	155.7	4.7	1.1	$203.7 \pm 8^{+52}_{-22}$	213	$7.5 \pm 0.3^{+0.2}_{-0.1}$	$12.9 \pm 0.8^{+1.2}_{-1.3}$
(6)	0.0	0.0	6.1	2.6	0.0	$8.7 \pm 1.6^{+1.3}_{-0.1}$	4	$3.5 \pm 0.2^{+0.2}_{-0.0}$	$3.4 \pm 0.4^{+0.4}_{-0.3}$
(7)	0.0	0.0	0.1	2.3	0.0	$2.9 \pm 0.4^{+0.1}_{-0.1}$	1	$3.1 \pm 0.2^{+0.2}_{-0.0}$	$3.3 \pm 0.4^{+0.4}_{-0.3}$

Table 4
$\mu\mu$ channel. Expected numbers of events for total background, signal points A and B, and number of observed events in data, in the 5 H_T bins. Statistical and JES uncertainties are added in quadrature for the total background and signal points

Bin	Total background	Data	Signal	
			Point A	Point B
$H_T \in]0, 40]$ GeV	0.11 ± 0.0	0	2.0 ± 0.3	0.5 ± 0.1
$H_T \in]40, 80]$ GeV	0.89 ± 0.4	0	1.1 ± 0.3	1.0 ± 0.1
$H_T \in]80, 120]$ GeV	0.75 ± 0.0	0	0.2 ± 0.1	0.8 ± 0.1
$H_T \in]120, 160]$ GeV	0.56 ± 0.0	1	0.0 ± 0.0	0.4 ± 0.1
$H_T \in]160, \ldots[$ GeV	0.57 ± 0.0	0	0.0 ± 0.0	0.4 ± 0.1

Table 3 summarizes the different stages of the signal selection in the $\mu\mu$ channel. The $t\bar{t}$ background dominates after the selection cuts; five H_T bins are considered (see Table 4) to separate various signal points from this background.

The expected numbers of background and signal events depend on several measurements and parametrizations which each introduce a systematic uncertainty: lepton identification and reconstruction efficiency [(2.6–7)%] [13], trigger efficiency [(3.5–5)%] [13], luminosity [6.1%] [15], multijet background modeling [10%], JES [(4–22)%] [12], jet identification and reconstruction efficiency and resolution [(4–16)%] [13], b jet tagging [(1–11)%] [16], PDF uncertainty affecting the signal efficiency [10%] [17].

After applying all selection cuts for $e\mu$ and $\mu\mu$ data sets, no evidence for $\tilde{t}_1$ production is observed. We combine the number of expected signal and background events and their corresponding uncertainty, and the number of observed events in data from the twelve bins of the $e\mu$ selection (Table 2) and the five bins of the $\mu\mu$ selection (Table 4) to calculate upper-limit cross sections for signal production at the 95% C.L. for various signal points using the modified frequentist approach [18]. In this calculation, correlated uncertainties are taken into account; no overlap is expected nor observed between the two samples. Regions for which the calculated cross section upper limit is smaller than the theoretical one are excluded at 95% C.L. Fig. 3 shows the excluded region as a function of the scalar top quark and sneutrino masses, for nominal (solid line) and for both minimal and maximal (band surrounding the line) values of the $\tilde{t}_1\bar{\tilde{t}}_1$ production cross section; the latter variation corresponds to the PDF uncertainty for the signal cross section, quadratically added to the $2\mu_r$ and $\mu_r/2$ renormalization scale variations of the $\tilde{t}_1\bar{\tilde{t}}_1$ cross section. Although the numbers of expected and

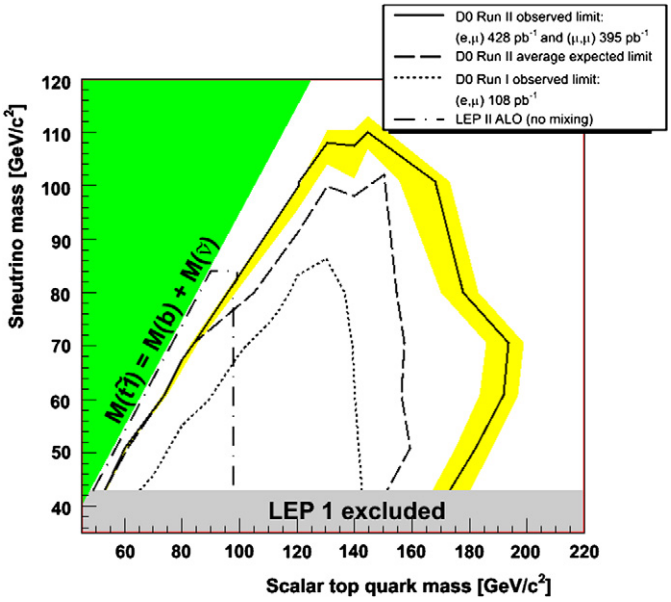

Fig. 3. For the nominal production cross section, the 95% C.L. excluded regions in the $[M(\tilde{t}_1), M(\tilde{\nu})]$ plane for the observed (full curve) and the average expected (dashed curve) limits are shown; the band surrounding the observed limit represents the lower and upper bounds of the signal cross-section variation. The regions excluded by D0 during Run I [14] and by LEP [19] are also shown.

observed events are similar (Tables 1 and 3), their distribution across the bins (Tables 2 and 4) causes the expected cross section limit to be lower than the observed one. For minimal values of the production cross section, the search in the $e\mu$ final state individually excludes a stop mass of 176 GeV/c^2 for a sneutrino mass of 60 GeV/c^2, and a sneutrino mass of 97 GeV/c^2 for a stop mass of 130 GeV/c^2; the search in the $\mu\mu$ final state,

once combined with the $e\mu$ final state, extends the final sensitivity by approximately 10 GeV/c^2 for small and large mass differences.

In summary, we have searched for the lightest scalar top quark decaying into $b\ell\tilde{\nu}$; events with an electron and a muon, and two muons have been considered for this search. No evidence for the lightest stop is observed in these decays, leading to a 95% C.L. exclusion in the $[M(\tilde{t}_1), M(\tilde{\nu})]$ plane. The largest stop mass excluded is 186 GeV/c^2 for a sneutrino mass of 71 GeV/c^2, and the largest sneutrino mass excluded is 107 GeV/c^2 for a stop mass of 145 GeV/c^2; these mass limits are obtained with the most conservative theoretical production cross section, taking into account the PDF uncertainty and the variation of the renormalization scale. This is the most sensitive search for stop decaying into $b\ell\tilde{\nu}$ to date.

Acknowledgements

We thank the staffs at Fermilab and collaborating institutions, and acknowledge support from the DOE and NSF (USA); CEA and CNRS/IN2P3 (France); FASI, Rosatom and RFBR (Russia); CAPES, CNPq, FAPERJ, FAPESP and FUNDUNESP (Brazil); DAE and DST (India); Colciencias (Colombia); CONACyT (Mexico); KRF and KOSEF (Korea); CONICET and UBACyT (Argentina); FOM (The Netherlands); Science and Technology Facilities Council (United Kingdom); MSMT and GACR (Czech Republic); CRC Program, CFI, NSERC and WestGrid Project (Canada); BMBF and DFG (Germany); SFI (Ireland); The Swedish Research Council (Sweden); CAS and CNSF (China); Alexander von Humboldt Foundation; and the Marie Curie Program.

References

[1] S.P. Martin, in: G.L. Kane (Ed.), Perspectives on Supersymmetry, World Scientific, Singapore, 1998, hep-ph/9709356.
[2] H. Hikasa, M. Kobayashi, Phys. Rev. D 36 (1987) 724.
[3] D0 Collaboration, V.M. Abazov, et al., Phys. Lett. B 645 (2007) 119.
[4] D0 Collaboration, V.M. Abazov, et al., Nucl. Instrum. Methods A 565 (2006) 463.
[5] A. Pukhov, et al., User's manual for version 3.3, INP-MSU 98-41/542.
[6] T. Sjöstrand, et al., Comput. Phys. Commun. 135 (2001) 238.
[7] M.L. Mangano, et al., JHEP 0307 (2003) 001.
[8] H.L. Lai, et al., Eur. Phys. J. C 12 (2000) 375.
[9] R. Hamberg, W.L. van Neerven, T. Matsuura, Nucl. Phys. B 359 (1991) 343;
R. Hamberg, W.L. van Neerven, T. Matsuura, Nucl. Phys. B 644 (2002) 403, Erratum;
J.M. Campbell, R.K. Ellis, Phys. Rev. D 60 (1999) 113006, hep-ph/9905386;
N. Kidonakis, R. Vogt, Phys. Rev. D 68 (2003) 114014;
U. Baur, E.L. Berger, Phys. Rev. D 41 (1990) 1476.
[10] R. Brun, F. Carminati, CERN Program Library Long Writeup W5013, 1993, unpublished.
[11] G.C. Blazey, et al., in: U. Baur, R.K. Ellis, D. Zeppenfeld (Eds.), Proceedings of the Workshop: QCD and Weak Boson Physics in Run II, Fermilab-Pub-00/297, 2000.
[12] D0 Collaboration, V.M. Abazov, et al., Phys. Rev. D 75 (2007) 092001.
[13] D0 Collaboration, V.M. Abazov, et al., Phys. Rev. D 76 (2007) 052006.
[14] D0 Collaboration, V.M. Abazov, et al., Phys. Rev. Lett. 88 (2002) 171802.
[15] T. Andeen, et al., The D0 experiment's integrated luminosity for Tevatron Run IIa, Fermilab-TM-2365, 2007.
[16] S. Greder, Ph.D. thesis, Fermilab-Thesis-2004-28, 2004;
B. Clément, Ph.D. thesis, Fermilab-Thesis-2006-06, 2006.
[17] J. Pumplin, et al., JHEP 0207 (2002) 012;
D. Stump, et al., JHEP 0310 (2003) 046.
[18] T. Junk, Nucl. Instrum. Methods A 434 (1999) 435.
[19] LEPSUSYWG, ALEPH, DELPHI, L3 and OPAL experiments, note LEPSUSYWG/04-02, http://lepsusy.web.cern.ch/lepsusy/Welcome.html;
ALEPH Collaboration, A. Heister, et al., Phys. Lett. B 537 (2002) 5.